

ENERGY FLOW CONSIDERATIONS, AN EDUCATIONAL TOOL TO CLARIFY AEROELASTIC PHENOMENA

Th. van Holten,

Faculty of Aerospace Engineering,

Delft University of Technology, Delft, the Netherlands

Abstract

The paper presents a semi-qualitative method to discover destabilizing couplings in aeroelastic systems, without actually solving the equations of motion.

Examples are given for three well-known instabilities, first classical pitch - flap flutter, and ground resonance.

The third example concerns the influence of stall effects on flap - lag coupling, which points out a few less well-known instability possibilities

1 Notations

$C_{d\alpha}$	=	drag gradient
$C_{l\alpha}$	=	lift gradient
C_{xy}	=	inertia product
I_x, I_y, I_z	=	inertia moments
m, M	=	lumped masses
α	=	angle of attack
β	=	flapping angle
γ	=	Lock number
δ	=	displacement of rotor centre, non-dimensionalized by R
ε	=	hub angle
ζ	=	lead-lag angle, positive in lead direction
θ	=	pitch angle
$v_\beta, v_\zeta, v_\theta$	=	natural frequencies, non- dimensionalized by Ω
ψ	=	azimuth angle
Ω	=	rotor angular speed

2 Introduction

In engineering education aeroelastic phenomena of rotors may serve as a good illustration of complex dynamic problems. Furthermore, the study of these phenomena is essential for the (small) group of students who want to specialize in aeroelasticity of rotorcraft.

The approach found in most of the well known textbooks (e.g. refs. 1 through 4) unfortunately often lacks a qualitative introduction which might give some

physical understanding and feeling for the fundamental causes of instabilities.

Physical feeling is nevertheless very important during the modeling phase, as well as during the later interpretation of analytical results. In an analytical solution one generally sees all the degrees of freedom - no matter how many are included in the model - taking part in the vibrations. It is by no means clear therefore, what the really relevant DOF's are whose coupling are "the core of the problem". As a consequence one often sees a tendency, especially amongst the inexperienced analysts, to include as many DOF's as practically manageable, or even an escape towards "blind" FEM-like approaches.

The paper describes a semi-qualitative approach which has been found to be useful in giving more insight.

The method is based on a consideration of intermodal energy flows. The system is likely to become unstable when several vibration modes mutually transfer energy into each other. This situation can be identified without actually solving the system equations. The intermodal energy flow method might be considered as a qualitative interpretation of the "force phasing matrix" (ref.1), but in contrast to the latter does not require the complete solution of eigenvectors.

3 The principles of energy flow inspection

The principles of the method are, briefly summarized:

1. The dynamical equations of the system are written as a set of second-order systems, where the coupling terms are considered as external excitations for each separate degree of freedom.
2. We assume "virtual" damping in each degree of freedom, such that an oscillation with constant amplitude results. The amount of virtual damping does not depend on the actual damping in the system, and may be either positive or negative.
3. Using the well-known characteristics of second-order systems, we determine in a qualitative way for each degree of freedom the phase of the response to the "external" excitations.
4. Next, we inspect whether there are any external excitations in phase with the velocity of the degree of freedom considered. If so, the coupling term which is represented by this excitation pumps energy into the degree of freedom.
5. If there are degrees of freedom which mutually pump energy towards each other, this indicates the possibility of instability.

The reasoning here is, that the added virtual damping must in such a case continuously dissipate energy in order to achieve a constant amplitude. If we would take away the virtual damping, and if the actual damping is less, then the mutual energy exchange would tend to increase the amplitude.

A simple example will first be shown in order to clarify the above procedure.

4 A simple example: pitch-flap flutter

We consider a rigid blade connected by a central flap and pitch hinge to the hub. The hinge-order is flap-pitch. A torsion spring realizes a non-rotating pitch frequency v_θ (non-dimensionalized by the angular speed $\Omega = d\psi/dt$).

The positive directions of the angles ψ (azimuth), β (flap), and θ (pitch) are indicated in fig.1.

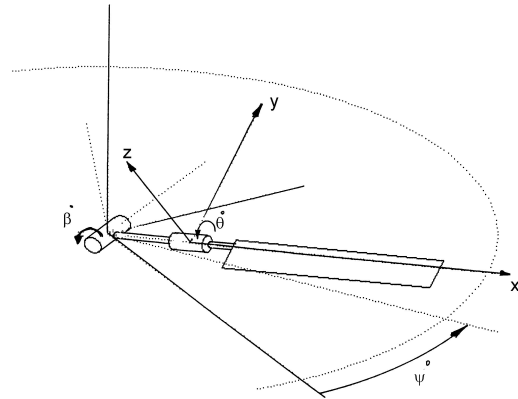


Figure 1: Pitch-Flap configuration

The blade is modeled as a thin lamina, with moments of inertia I_x, I_y, I_z and only one product of inertia C_{xy} , where the X-axis lies along the c/4-line of the blade, and the Y-axis points forward in chordwise direction. Quasi-steady, linear aerodynamics is assumed.

The linearized perturbation equations, retaining only the most important terms, are:

$$C_{xy}^* (\beta'' + \beta) + \theta'' + (1 + v_\theta^2) \theta = 0$$

$$\beta'' + \frac{\gamma}{8} \beta' + \beta - \frac{\gamma}{8} \theta = 0$$

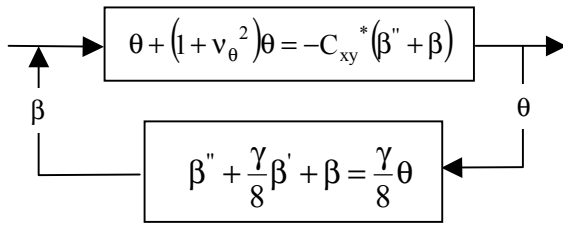
where

$$C_{xy}^* = C_{xy} / I_x$$

$$\gamma = \frac{\rho C_{l\alpha} c R^4}{I_y} \quad (\text{Lock number})$$

and the notations '' and '' indicate derivatives with respect to the non-dimensional time ψ .

For the purpose of an energy-flow inspection we rearrange these equations as shown in the following block-diagram:



Now we assume "virtual" damping in the system so that it will oscillate with a constant amplitude. The non-dimensional oscillation frequency is ν , with $\nu > 1$ if there is a positive spring-stiffness in the pitch degree of freedom, i.e. $(1 + \nu_\theta^2) > 1$.

Let us assume that the resulting oscillation in pitch is proportional to $\cos \nu \psi$:

$$\theta \sim \cos \nu \psi$$

The excitation of the flapping degree of freedom β , given by the term $\gamma/8 \theta$ is thus proportional to $\cos \nu \psi$. Because the excitation frequency is higher than the natural frequency of the flap motion, the response of the flapping angle β will be shifted in phase, and will be proportional to:

$$\beta \sim (1 - \epsilon) \sin \nu \psi - \epsilon \cos \nu \psi$$

If the excitation frequency ν is close to 1, i.e. close to the natural frequency of the flap motion, the response will be nearly $\pi/2$ out of phase with the excitation. In that case $\epsilon = 0$.

On the other hand, if the excitation frequency is much higher than the flap frequency, the response will be nearly in antiphase, and $\epsilon = 1$.

We conclude that in the general case there is energy transfer from the pitching motion to the flapping motion since the flapping velocity

$$\beta' \sim (1 - \epsilon) \cos \nu \psi + \epsilon \sin \nu \psi$$

contains terms that are in phase with the excitation

$$\frac{\gamma}{8} \theta \sim \cos \nu \psi$$

The response of the flapping angle causes in turn an external excitation of the pitch motion, through the coupling term

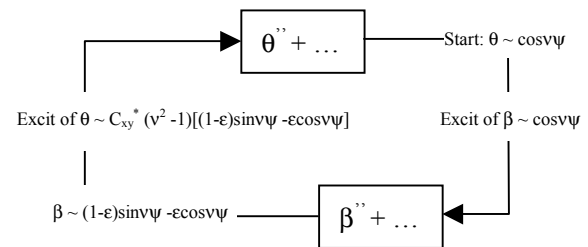
$$-C_{xy}^* (\beta'' + \beta) \sim C_{xy}^* (\nu^2 - 1) [(1 - \epsilon) \sin \nu \psi - \epsilon \cos \nu \psi]$$

On condition that $C_{xy} < 0$ (centre of gravity of the blade behind the c/4-line) there is energy transfer from the flapping motion back to the pitching motion, since the coupling term $-C_{xy}^* (\beta'' + \beta)$ in that case contains a part which is in phase with the pitching velocity

$$\theta' \sim -\sin \nu \psi$$

The condition of the two degrees of freedom mutually pumping energy into each other is thus satisfied if the centre of gravity lies behind the c/4-line, and under this condition instability may thus occur.

The complete picture is summarized in the following diagram:



There exist two limiting cases where the energy cycle is no longer closed, as follows from the above shown diagram:

- 1 If the torsion spring constant is zero, then the frequency of the oscillation will become $\nu = 1$, and the coupling term from flap to pitch vanishes.
- 2 If the torsion spring is very stiff, the torsion frequency will be very far removed from the natural frequency of the flapping motion. In that case the flapping response will be mainly in anti-phase with its excitation ($\epsilon \rightarrow 1$). Integrated over one oscillation cycle, the product $\gamma/8 \theta \beta'$ will be zero, and again the energy cycle is broken.

The conclusions from these energy flow considerations are fully in agreement with the well-known results for

simple flap-pitch instability. Fig. 2 shows the general character of the stability boundary as derived in the literature, see e.g. ref.3.

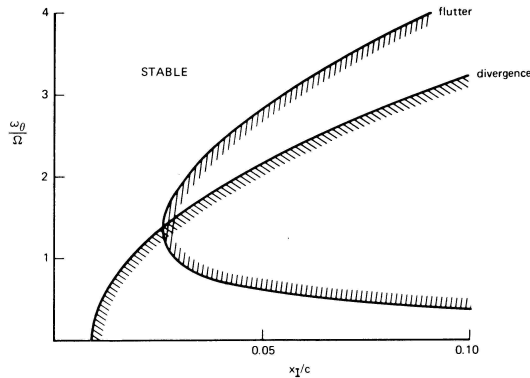


Figure 2: General character of pitch-flap flutter boundary

5 Flap-lag—stall instability

A more interesting case will now be presented, viz. the stability of a rotor with flap- and lag degrees of freedom, influenced by stall. The case is interesting because the energy flow inspection shows several destabilizing factors which are often neglected in the well known textbooks. These potential instabilities may be important in practice, especially in the case of large windturbine rotors.

The aeroelastic model is shown in fig.3. The angles describing the instantaneous position of a blade are:

- ψ : azimuth angle of the constant speed shaft. This angle is also used as non-dimensional time.
- ε : the hub angle with respect to the constant speed shaft. The hub spring is chosen to represent multiblade effects. In the case of symmetric lagging modes, the hub spring is taken infinitely stiff, whereas asymmetric modes are represented by a relatively low clamping stiffness.
- θ : the so-called structural coupling angle. It measures the rotation of the axis of least bending stiffness of the blade with respect to

the hub axis: the so-called "flatwise" direction in contrast to the pure flapwise direction perpendicular to the plane of rotation. The angle θ therefore represents both the pitch setting as well as the effect of structural twist of the blade. θ is taken to be constant.

- ζ : the lead-lag angle of the blade, positive in lead-direction. Again this angle is taken in "edgewise" direction instead of purely parallel to the plane of rotation.
- β : the flapping angle of the blade (flatwise). A wind turbine situation is considered, with β taken positive in the same direction as the undisturbed flow.

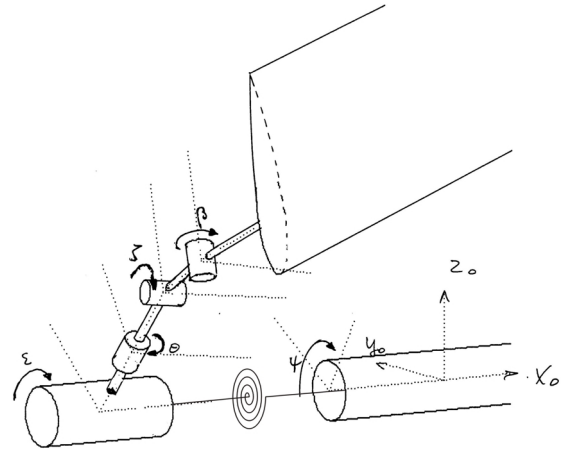


Figure 3: Flap-Lag configuration

Although central hinges are assumed, there is a definite hinge order: hub - lag - flap.

The aerodynamic model comprises quasi-steady stall as shown in fig.4 (lift) and 5 (drag). The lift and drag gradients of a section are determined by local linearization around the angle of attack associated with the steady equilibrium state of the rotor. The steady state is indicated as C_{l0} , α_0 and C_{d0} . In the non-linear region of the lift curve, the local lift gradient is denoted as $C_{l\alpha}^*$, and a similar notation $C_{d\alpha}^*$ is used for the drag.

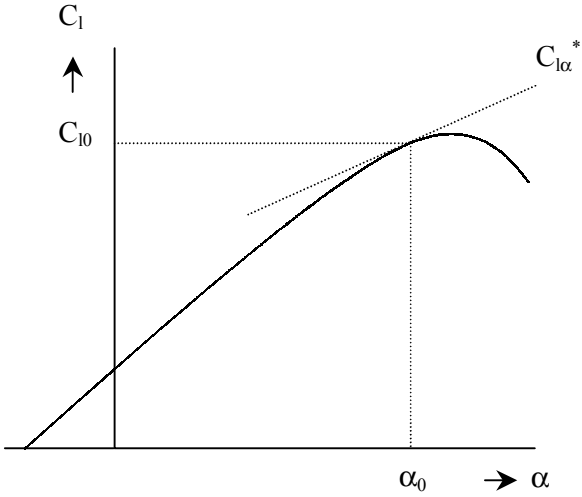


Figure 4: Linearization of non-linear lift-characteristics

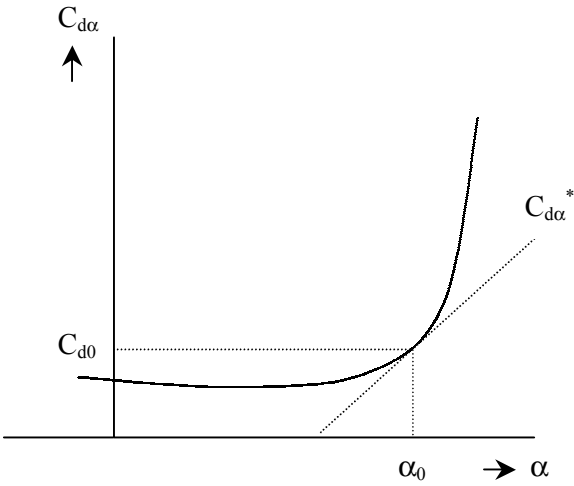


Figure 5: Linearization of non-linear drag-characteristics

A "representative section" model is used, i.e. the flow angles at the 3/4-radius position are taken to be representative for the conditions along the entire blade. Note however, that the variation along the span of the absolute magnitude of the velocities is taken into account.

The full derivation of the equations of motion is given in ref.5. The resulting semi-linearized perturbation equations are:

Hub equation:

$$\beta'' \sin \theta + \left[-2\beta_0 + \frac{\gamma(C_{l0} - C_{d\alpha}^*)}{8C_{l\alpha}} \right] \beta' + \varepsilon'' + \frac{\gamma}{8C_{l\alpha}} 2C_{d0} \varepsilon' + v_\varepsilon^2 \varepsilon + \zeta'' \cos \theta + \frac{\gamma}{8C_{l\alpha}} 2C_{d0} \zeta' = 0$$

Lag equation:

$$\left[-2\beta_0 + \frac{\gamma(C_{l0} - C_{d\alpha}^*)}{8C_{l\alpha}} \right] \beta' + \varepsilon'' \cos \theta + \frac{\gamma}{8C_{l\alpha}} 2C_{d0} \varepsilon' + \zeta'' + \frac{\gamma}{8C_{l\alpha}} 2C_{d0} \zeta' + v_\zeta^2 \zeta = 0$$

Flap equation:

$$\beta'' + \frac{\gamma^*}{8} \beta' + (1 + v_\beta^2) \beta + \varepsilon'' \sin \theta + 2 \left[\beta_0 - \frac{\gamma}{8C_{l\alpha}} C_{l0} \right] (\varepsilon' + \zeta') = 0$$

where γ^* denotes the Lock-number based on the non-linear lift gradient.

In most textbooks just one possible flap - lag instability is treated. However, an energy flow inspection shows that there are in fact 5 different ways in which the energy flow loops can be closed. Let us first consider the most well-known loop closure which may be found in most text books.

5.1 Case 1: "classical" flap-lag instability.

In this case it is assumed that the drag gradient is nearly zero: $C_{d\alpha} = 0$. The steady state equilibrium condition yields a relation between C_{l0} and the equilibrium coning angle β_0 :

$$\beta_0 (1 + v_\beta^2) = \frac{\gamma C_{l0}}{8C_{l\alpha}}$$

so that the flapping equation may be written in the simplified form:

$$\beta'' + \frac{\gamma^*}{8}\beta' + (1 + v_\beta^2)\beta = 2\beta_0 v_\beta^2 (\epsilon' + \zeta') - \epsilon'' \sin \theta$$

It may be seen that in the case of no flapping spring stiffness the lag velocity ζ' (and likewise ϵ') do not influence the flapping motion. The reason is simple: a lagging velocity will affect the centrifugal moment on the blade by exactly the same amount as it affects the aerodynamic moment.

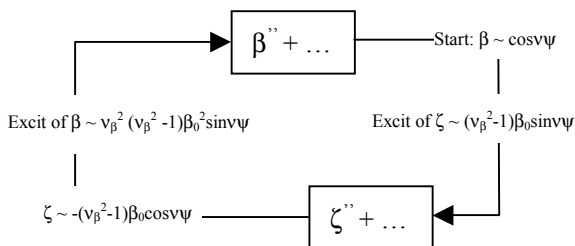
There is still some coupling with the hub motion through the term $\epsilon'' \sin \theta$: a rotational acceleration of the hub causes "d'Alembert inertial forces" on the blade which have a component in flap direction (or rather: the flatwise direction) because of the pitch setting and twist of the blade.

Similarly, the other equations are simplified to read, neglecting the influence of drag:

$$\zeta'' + v_\zeta^2 \zeta = -(v_\beta^2 - 1)\beta_0 \beta' - \epsilon'' \cos \theta$$

$$\epsilon'' + v_\epsilon^2 \epsilon = -(v_\beta^2 - 1)\beta_0 \beta' - \beta'' \sin \theta - \zeta'' \cos \theta$$

For simplicity we assume that all the natural frequencies coincide, so that the three DOF's are all excited exactly in their resonance frequency, which is accompanied by phase shifts of exactly $\pi/2$. The resulting energy flow diagram looks like:



It is concluded that the energy flow loop is closed for $0 < v_\beta^2 < 1$, i.e. if the non-dimensional rotating flapping frequency lies in the range $1 < v_{\beta r} < 1.4$. This agrees with the classical theory on flap-lag instability, see e.g. fig.6 taken from ref.3.

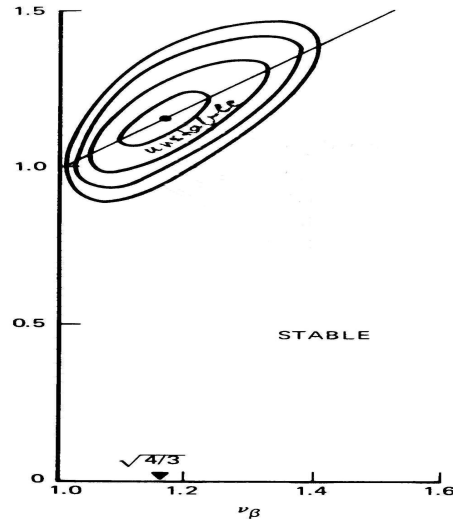


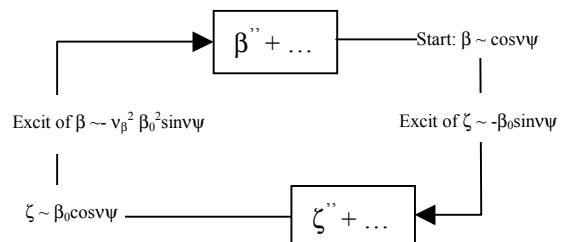
Figure 6: Classical flap-lag instability

Looking back at the origin of the term $(v_\beta^2 - 1)\beta_0$, one sees that the main destabilizing effect is the Coriolis force on the blade due to a flapping velocity. A stabilizing effect originates from the tilting of the liftvector due to the flapping velocity.

This immediately points out another danger of instability. In the above given derivation the drag gradient $C_{d\alpha}$ was neglected. In the non-linear pre-stall region the value of $C_{d\alpha}$ grows, and diminishes the tilting of the resultant aerodynamic force due to a flapping velocity. Near the stall, the stabilizing tilting effect may become small or may vanish completely (see e.g. ref.6) so that the destabilizing Coriolis effect dominates. This leads to case 2 of the series of possible instabilities.

5.2 Case 2: "drag stall"

In order to simplify the analysis, let us assume that due to drag stall the Coriolis effect due to flapping dominates, so that in the equations of motion the term $-(v_\beta^2 - 1)\beta_0 \beta'$ tends to $-(v_\beta^2 - 1)\beta_0 \beta' \rightarrow 2\beta_0 \beta'$. In this case, again assuming that the natural frequencies coincide, the energy flow diagram becomes:



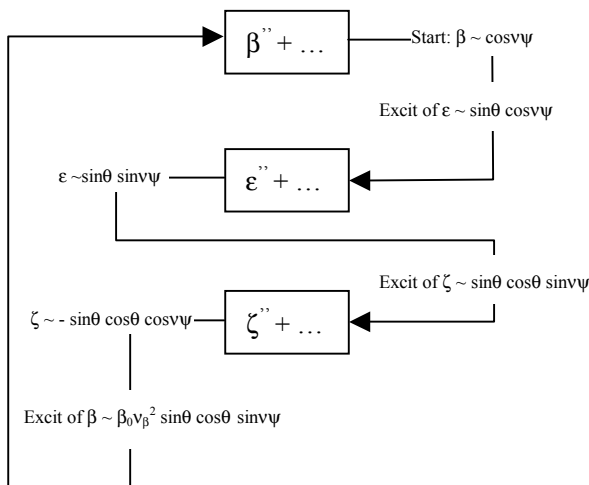
This may be a relatively strong instability, since near the stall also the liftgradient $C_{l\alpha}$ decreases, so that the diminishing aerodynamic damping in the flapping motion further aggravates the problem. Presently it is thought (see ref.7) that this instability is a main contributor to the severe lag vibrations which have been observed in large wind turbines (diameter 50 m or larger). Due to scale effects, in the case of windturbines the flap and lag frequencies tend to approach each other with increasing diameter.

5.3 Cases 3 and 4: Coupling with hub motion

In the rotor model presented, closed energy loops may similarly occur between the flap and hub degree of freedom, analogous to cases 1 and 2. The equivalent hub stiffness in the one-blade model depends among other factors on multi-blade effects. The relation between the equivalent hub stiffness of the one-blade model and the real rotor stiffnesses is treated in ref.8. It is difficult to make general statements about the severity of these potential destabilizing effects.

5.4 Case 5: 3-DOF instability, involving blade twist effects.

In this case we concentrate on the remaining terms in the equations of motion, representing "d'Alembert couplings" like $\beta'' \sin\theta$ and $\epsilon'' \cos\theta$, in combination with the term $2\beta_0 v_\beta^2 \zeta'$ which is the aerodynamic flapping moment due to an increase of the rotorspeed. A closed loop energy flow appears to be possible as sketched in the following diagram:



The conclusion is, that for $\theta < 0$ (corresponding to positive pitch in helicopter convention !) a closed

energy loop is possible. It must be emphasized that this loop closure is only then possible if all three the degrees of freedom can take part in the oscillation. This excludes the case where a symmetric multiblade lag mode is involved. In the case of stiff inplane tailrotors the effect may certainly contribute a destabilizing effect.

6 Rotor - chassis resonances

The third example shows a slightly more pictorial way of explaining dynamic interactions. The example concerns the coupling of the lag motion with chassis motions. From the usual analyses in the textbooks it follows that the advancing lag-mode cannot become unstable, and that only the ground resonance case is potentially dangerous. However, the energy flow considerations point out that there may be cases where the advancing lag mode does contribute to unstable chassis motions, viz. when certain inplane forces are involved. This coupling is therefore important for wind turbines where gravity may play an important role. At least one case of wind turbine instability has been caused by this phenomenon.

The following simplified model is used (fig.7). It consists of a constant speed shaft (angular velocity Ω) which may translate w.r. to an inertial frame (the non-dimensional translation coordinate is δ). A hub is connected to the shaft by means of a torsion spring, so that the hub may have a variable angular velocity $\Omega(1 + \zeta')$. To the hub is attached a massless beam with a concentrated mass at its end. In order to balance the average centrifugal force, a counterweight is attached to the constant speed shaft.

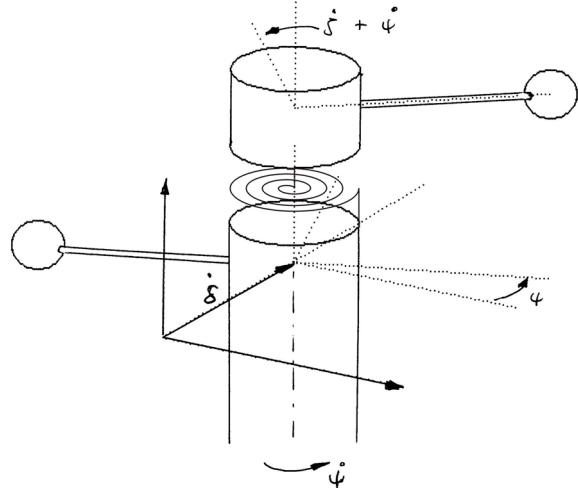


Figure 7: Ground resonance model

The equation of motion for the translation is:

$$\delta'' + v_\delta^2 \delta = m^* [\zeta \cos \psi + 2\zeta' \sin \psi - \zeta'' \cos \psi]$$

where

$$m^* = \frac{m}{(2m + M)},$$

m = lumped mass on beam, M = hub mass

The physical meaning of the terms on the r.h.s. is clear:

- $\zeta \cos \psi$ is associated with the unbalance of the centrifugal forces caused by a non-zero lead-angle.
- $2\zeta' \sin \psi$ is caused by the increase of the centrifugal force due to a lead-velocity
- $\zeta'' \cos \psi$ is the component of the "d'Alembert" inertia force due a lead-lag acceleration.

The equation of motion in lagging direction is:

$$\zeta'' + v_\zeta^2 \zeta = -\delta'' \cos \psi$$

Again, the nature of the "forcing" term on the r.h.s. is clear: a translatory acceleration causes "d'Alembert" inertia forces on the blade, and thus a moment around the shaft.

First of all we consider the usual ground resonance situation, see fig.8, point B.

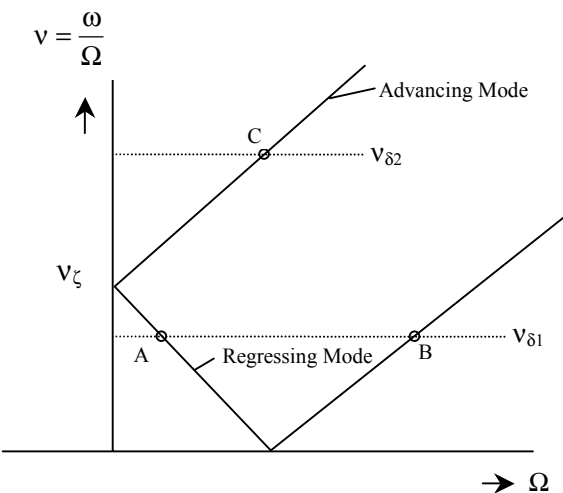


Figure 8: Principle diagram ground resonance

We assume for simplicity that the crossing of the chassis frequency with the regressing lag-mode occurs at the non-dimensional frequencies $v_\delta = v_\zeta = 1/2$:

$$\zeta = \zeta_0 \cos(\psi / 2)$$

The situation is depicted in fig.9a. Each lead-lag cycle takes two rotor revolutions. From the physical meaning of the forcing terms acting on the chassis it is clear that at $\psi = 0$, where maximum lead occurs, a force will be exerted on the chassis to the right. One revolution later, at $\psi = 2\pi$ maximum lag occurs with an attendant force on the chassis to the left, etc. If it is wished, this may be checked easily by substituting $\zeta(\psi)$ into the equations of motion.

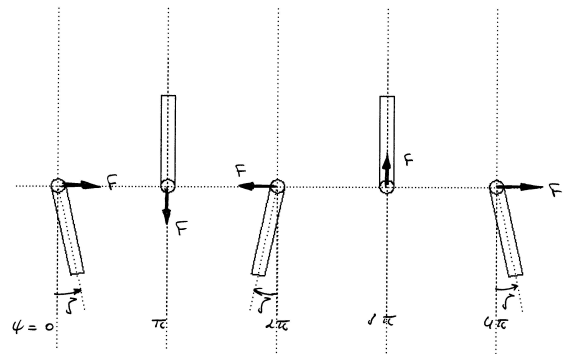


Figure 9a: Chassis forces due to lead-lag

The chassis is excited in its natural frequency, so that its response will show a phase difference with respect to the applied force, as sketched in fig.9b. The maximum positive chassis displacement thus occurs at $\psi = \pi$, and a maximum deflection to the left is found at $\psi = 3\pi$. This movement is associated with maximum accelerations of the chassis at $\psi = \pi$ and at $\psi = 3\pi$, in a direction opposite to the deflections. The resulting "d'Alembert" lead-lag moments on the blade are also shown in fig.9b, and it is seen that these moments are in phase with the lead-lag velocity.

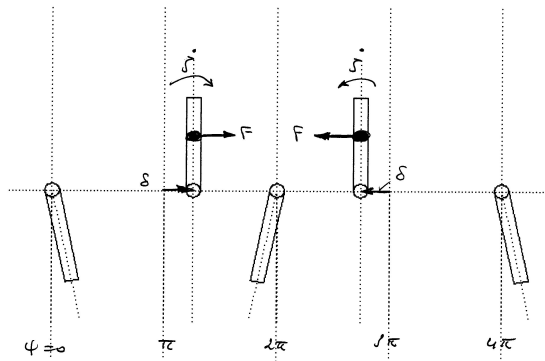


Figure 9b: Chassis displacement and moments on blade

The complete picture shows that there is a positive energy flow from the lag motion to the chassis motion, and vice versa. This mutual energy "pumping" indicates the possibility of instability, which explains the occurrence of ground resonance if the damping in the system is insufficient.

Using the energy flow method, one may also explain why damping should be used both in the rotor system and in the chassis, whereas damping in just one of the coupled DOF's is ineffective. Furthermore, similar considerations explain why the low speed crossing point of the chassis frequency with the regressing mode (fig.8, point A) cannot show unstable behaviour. For the sake of brevity these subjects will not be elaborated further.

In the ERF-paper "The influence of scale effects on the aeroelastic stability of large wind turbines" (ref.7) it is shown by similar energy flow considerations that gravity effects may cause unstable behaviour at point C of fig.8. This is the crossing point of the chassis frequency with the advancing mode, which is usually considered to be stable under all normal circumstances met in the case of helicopters.

7 Conclusions

The energy flow method, although it is mainly qualitative, is nevertheless a relatively powerful tool to explain aeroelastic phenomena, and to give a feeling for the most important factors involved.

The examples given (classical binary flutter, flap-lag-stall and ground resonance) show that such qualitative considerations may even point out instability possibilities which are usually not mentioned in the

textbooks, but may in practice indeed occur under certain special circumstances.

8 References

1. R.L. Bielawa, Rotary wing Structural dynamics and Aeroelasticity, AIAA Education Series, Copyright by the American Institute of Aeronautics and Astronautics Inc., Washington DC, 1992.
2. A.R.S. Bramwell, Helicopter Dynamics, Edward Arnold (Publishers) Ltd., London WC1B3DQ, 1976
3. W. Johnson: Helicopter Theory, Princeton University Press, Princeton , New Jersey, in 1980
4. R.W.Prouty: Helicopter Performance, Stability, and Control, Robert E. Krieger Publishing Company, Malabar, Florida 1990
5. Th. Van Holten, J.G. Holierhoek, Th.J. Mulder, Flap-Lag-Stall Analysis of large Wind Turbines, Flight Mechanics & Propulsion Group, Delft University of Technology, to be published as contractor report to NOVEM.
6. L.A. Viterna, R.D. Corrigan: Fixed pitch rotor performance of large horizontal axis wind turbines, NASA CP 2230, Cleveland 1981.
7. Th. Van Holten, M.D. Pavel , G.N. Smits, The Influence of Scale Effects on the Aeroelastic stability of Large Wind Turbines, paper no. 71, 26th European Rotorcraft Forum, The Hague, September 2000.
8. Th. Van Holten, Th.J. Mulder, Hub Stiffness as Influenced by Multi-Blade Effects, Flight Mechanics & Propulsion Group, Delft University of Technology, to be published as contractor report to NOVEM.